International Journal of Electronics Communication and Computer Engineering
Volume 5, Issue 5, ISSN (Online): 2249–071X, ISSN (Print): 2278–4209

A Novel ANFIS Net for Classifying Features from Remotely Sensed Images

G. M. Behery
Faculty of Science, Damietta University

***Abstract* – This article presents a novel adaptive neuro-fuzzy inference system (ANFIS) net that is designed to classify dust, clouds, water and vegetation features from remotely sensed images. This system can reestablish the architecture of the ANFIS net according to a linear combination among the kind of membership function (MF), the number of MF, and number of epochs in automatic way. The proposed system is trained on the features of the provided images using eight kinds of MFs, and is designed to find the best ANFIS net that has the ability to have the best classification on data is not included in the training data. This system shows an excellent classification of test data that is collected from the training data. The performances of the best three MFs are %98.95, %98.72 and %98.62 for test data that is not included in the training data. Although, the proposed system was trained on data selected only from one image, this system shows correctly classification of the features in the all images. The designed system can be carried out on remotely sensed images for classifying other features.**

***Keywords* – ANFIS, Image Processing, Classification, Features.**

I. INTRODUCTION

Jang [1], [2] combined both Fuzzy Logic and artificial neural networks to produce a powerful processing tool, named ANFIS. ANFIS uses an artificial neural network learning algorithm to set fuzzy rule with the appropriate MFs from input and output data. Actually, this technique is an appropriate solution for function approximation in which a hybrid learning algorithm applied for the shape and the location of MFs [3], [4]. Moreover, a practical example of this method was introduced in [5]-[7].

The integration of remote sensing techniques and connectionist models for the prediction of fishing banks is presented [8], [9]. Extraction of land-cover map information from multispectral or hyperspectral remotely sensed images is one of the important tasks of remote sensing technology [10]-[12]. Precise information about the landuse and land cover changes of the Earth's surface is extremely important for any kind of sustainable development program [13], [14]. The results of the neuro-fuzzy model using remote-sensing data and geographic information system for landslide susceptibility analysis in a parts of the Cameron Highlands and the Klang Valley areas in Malaysia are manifested [15]-[19]. Several configurations in the particular context of remote sensing for land cover are reviewed [20].

In order to automatically generate such landuse map from remotely sensed images, various pattern recognition techniques like classification and clustering can be adopted [21], [22]. These images are used in many applications e.g. for detecting the change in ground cover [23]-[25], extraction of forest [26]-[28], and others [29]-[31]. With the concepts and methods, applications of soft computing in the field of agricultural and biological engineering are presented especially in the soil and water context for crop management and decision support in precision agriculture [32]. There are primarily two approaches to estimating vegetation parameters such as leaf area index. The first one is associated with computation of spectral vegetation indices from radiometric measurements [33], [34].

Many techniques are applied based on ANFIS net. Some of them are adaptive neural-fuzzy-based multi-sensor data fusion architecture for target tracking systems [35], landuse susceptibility maps [36]-[38], evidential reasoning based on Dempster-Shafer theory [39], [40], nonlinear technique to improve the first guess using simulated infrared brightness temperatures [41], the fuzzy-Artificial immune recognition system system was used as a classifier in the diagnosis of lymph diseases [42], [43], the immune-based symbiotic particle swarm optimization [44], [45].

In this work, a novel ANFIS system is used for classifying four features from red sea area. The proposed system is systematically designed to work as dynamic classifiers using the following MFs. These functions are difference of two sigmoid (dsigmf), two-sided Gaussian curve (gauss2mf), Gaussian curve (gaussmf), generalized bell curve (gbellmf), Pi-shaped curve (pimf), product of two sigmoidal (psigmf), trapezoidal (trapmf), and triangular (trimf) MFs [46]-[48]. The rest of paper is organized as follows; Section 2 describes the pattern data that is used for training and testing the system. Section 3 presents the proposed system. Section 4 shows the obtained results. Finally, Section 5 concludes the work.

II. REMOTELY SENSED DATA

This study is carried out on three images that were obtained by the Moderate Resolution Imaging Spectroradiometer (MODIS) on NASA's Aqua satellite. The first image contains multiple dust plumes blew eastward across the Red Sea. Along the eastern edge of the Red Sea, some of the dust forms wave patterns. Over the Arabian Peninsula, clouds fringe the eastern edge of a giant veil of dust. East of the clouds, skies are clear. Along the African coast, some of the smaller, linear plumes in the south may have arisen from sediments near the shore, especially the plumes originating in southern Sudan. The wide, opaque plume in the north, however, may have arisen farther inland, perhaps from sand seas in the Sahara [49]; see Fig. 1. The second one has dust plumes blew off the coast of Africa and over the Red Sea. The dust

blowing off the coast of Sudan is thick enough to completely hide the land and water surface below, but the thickest dust stops short of reaching Saudi Arabia. Farther south, between Eritrea and Yemen, a thin dusty haze hangs over the Red Sea [50]; see Fig. 2. The third contains dust plumes blew off the coast of Sudan and across the Red Sea. Two distinct plumes arise not far from the coast of Sudan and blow toward the northeast. The northern plume almost reaches Saudi Arabia. North of these plumes, a veil of dust with indistinct margins extends from Sudan most of the way across the water [51]; see Fig. 3. These three images are called *image1*, *image2*, and *image3* respectively. They are RGB format and their information is shown in Table 1.

In this study, the classification is specified for dust, clouds, water, and vegetation features. Each feature has approximately the same color in the three images. So, the pattern data is selected randomly by sampling throughout the *image2* only. Where, it contains all features clearly. The selection of this data is such that it contains samples of all features. The pattern data for each pixel consists of three pixel grey-levels, one for each layer. These layers are red, green and blue. The grey levels in the original images are coded as eight bits binary numbers in the range from 0 to 255. In order to train the ANFIS net, all pixels values are normalized to lie between 0.0 and 1.0.The pattern data is collected from the proposed image for these features. After the collection, each feature is represented as one group. Each group is divided into two parts: two-thirds for training and one third for test. Then, the training groups are merged in single file, and the test groups in other file.

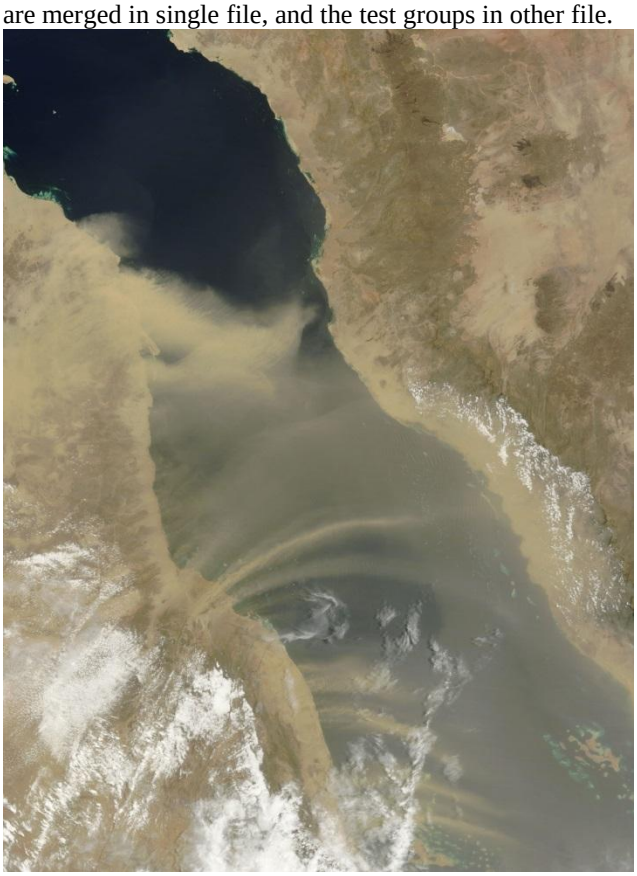

Fig.1. The first original image (image1) was taken by MODIS NASA's Aqua Satellite.

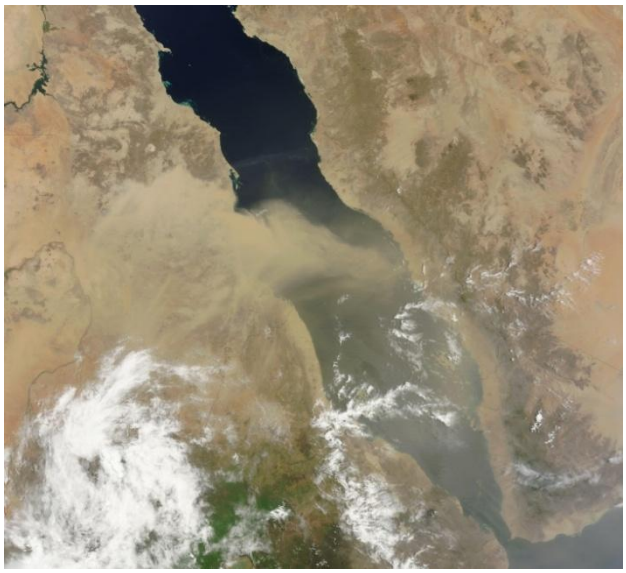

Fig.2. The second original image (image2) was taken by MODIS NASA's Aqua Satellite.

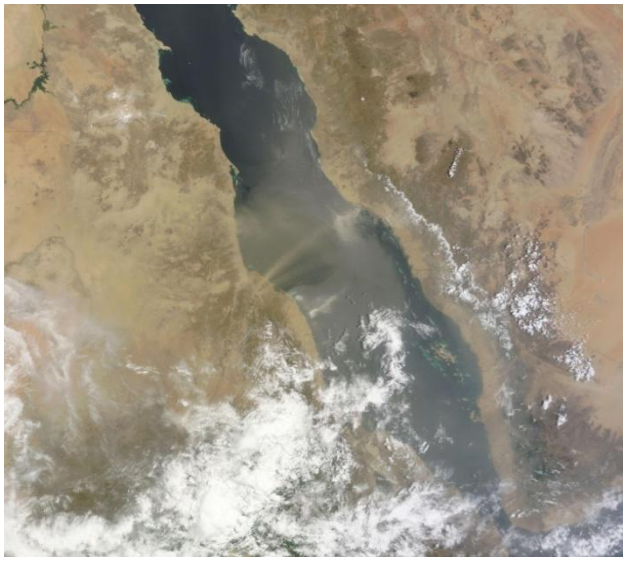

Fig.3. The third original image (image3) was taken by MODIS NASA's Aqua Satellite.

Table 1: Information of the studied three images

Name	taken date	length	width	size /MB
image1	July 24, 2010	4000	2800	1.14
image2	mid-July 2011	5916	6372	3.14
image3	Aug. 3, 2011	5916	6372	3.25

III. PROPOSED SYSTEM

ANFIS systems are very effective methods to classify features from remotely sensed images. Fig. 4 shows the ANFIS architecture. This architecture implements a TokagiSugeno FIS having a five layered architectures as shown in Fig. 5. The first layer represents fuzzy MF. The second and the third layers contain nodes that form the antecedent parts in each rule. The fourth layer calculates the first-order Takagi-Sugeno rules for each fuzzy rule. The fifth layer is the output layer, which calculates the weighted global output of the system [52].

The proposed system is designed to work in automatic way without any help from the user. The system is firstly started with building initial ANFIS architecture by selecting the first kind of MF from list, the number of MFs for each input, and the number of epochs. After that, the system is trained and tested. Then, the current training and test performances are reserved in two variables as the best train and test respectively, and the workspace is stored. After that, the system rebuilds the architecture of the ANFIS net according to a linear combination among MF names, number of MFs for each input, and number of epochs. When the system is reached the specified best training (B_train) and test (B_test) performances, the classification function is applied. In the case if the required performances are not reached, the system ask the user for enhancement the train and test data or adding new MF to the system. This improvement is carried out by removing the repeated and extreme pixels from all features. This new MF is designed by the user. And then retrain the system again. This system is illustrated in more details in the following algorithm and Figs. 6 and 7.

1 - Preprocessing
- *Create a list for kind of MFs.*
- *Specify the following components of ANFIS system.*
- *name of MF.*
- *number of MFs for each input*
- *number of epochs*
- *B_train, B_test, Max_number_mf, and Max_epochs*
- *current_mf_no = 1*

2- Build ANFIS architecture.
3- Train the system.
4- Do:
- *best train performance = Training performance;*
- *best checked performance = checked performance;*
- *save workspace.*

5- For MFs name = current_mf_no : length of the list
For number of MFs = 2 :Max_number_mf
For number of epochs = initialValue : Step: Max_epochs
- *build a new ANFIS system architecture;*
- *train the system;*
- *if (the Training performance >B_train and checked performance >B_test) go to step 8*
- *if (train performance > best training performance and checked performance > best checked performance)*
- *best train performance =Training performance;*
- *best checked performance = checked performance;*
- *save workspace;*
- *End if*

Next for
Next for
Next for

6- If you need to enhance the train and test data; call Enhancement_data function and then go to step 1.
7- If you need to add a new MF to the list of MFs names; add new MF; update the length of the list; current_mf_no = the length of the list, and then go to step 5.
8- Saves the workspace.
9- Call the classification process to extract features of partial images; see Fig. 6
10-Prints the results system and keep it in the files.
11-Stop.

***Function K = Enhancement_data** (actual_output_vector, tarjet_output_vector)*
For I =1: length of tarjet_output_vector
If (absolute(actual_output_vector(i)- tarjet_output_vector(i))>Max_error)
Remove the row number I from the training_data file
Next for
K = the enhanced train_data_file
End function

***Function y = new_MF_name** (arguments)*
Build the body of the new MF
Y = the mathematical form of that MF
End function

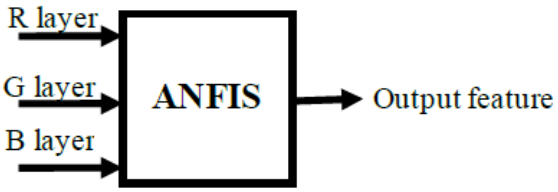

Fig.4. ANFIS net diagram

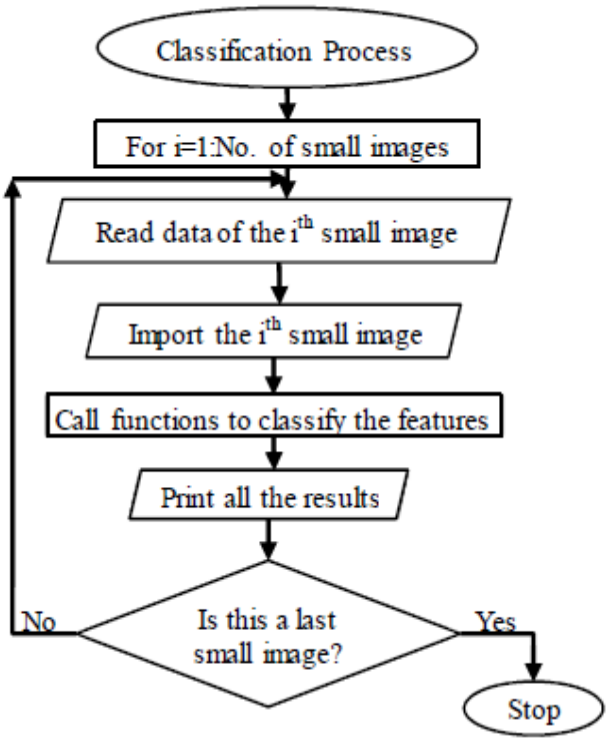

Fig.6. The proposed classification process

International Journal of Electronics Communication and Computer Engineering
Volume 5, Issue 5, ISSN (Online): 2249–071X, ISSN (Print): 2278–4209

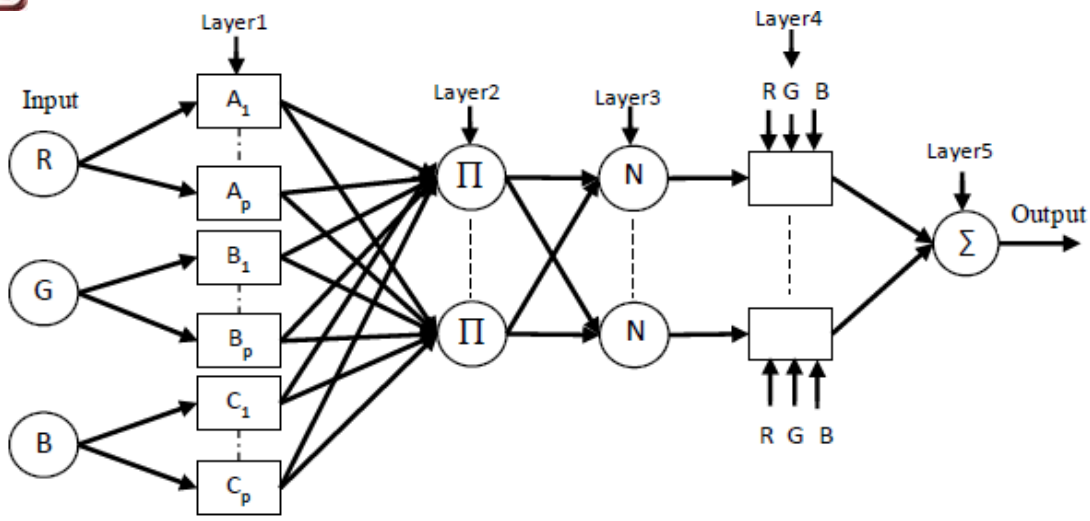

Fig.5. ANFIS net architecture.

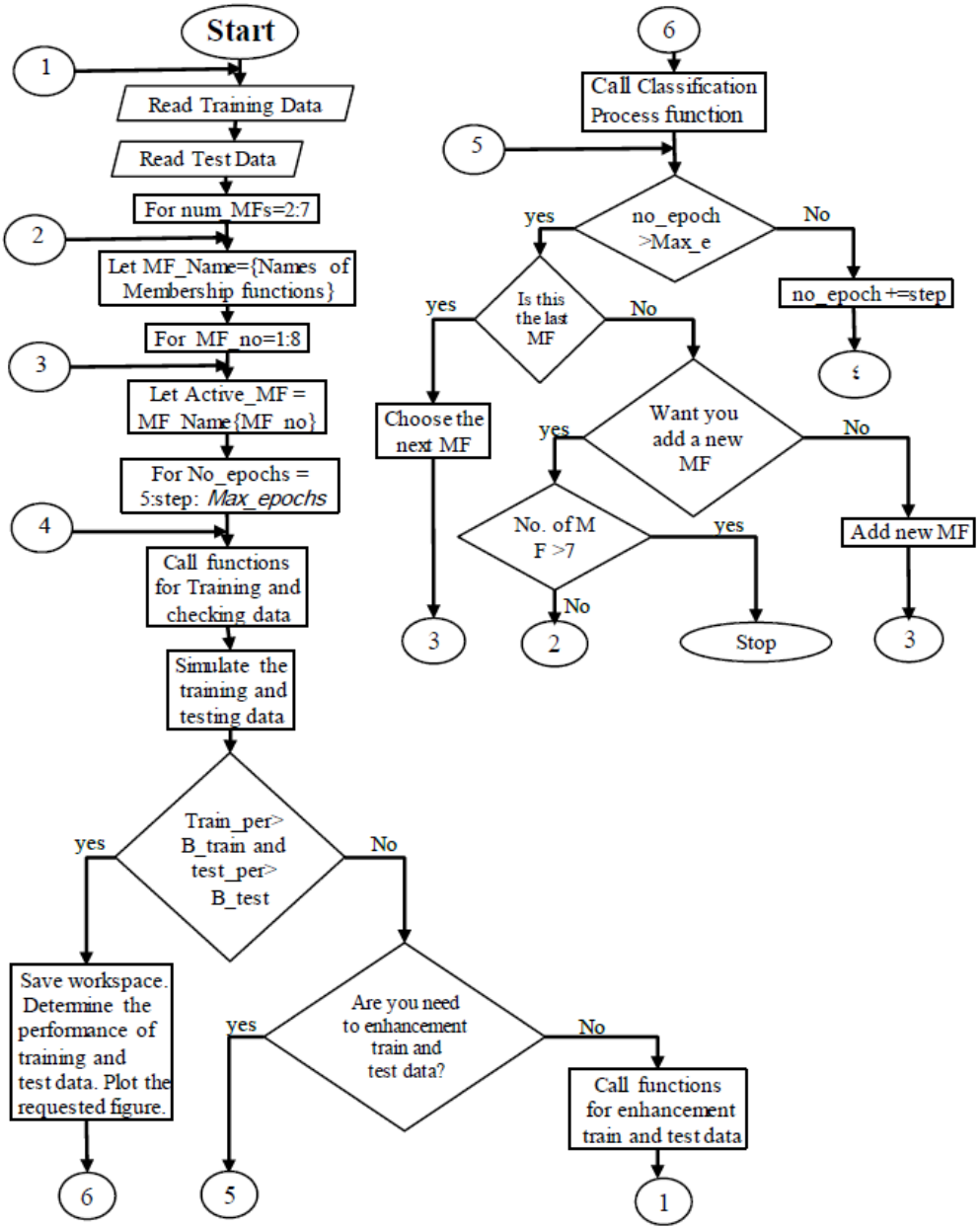

Fig.7.

International Journal of Electronics Communication and Computer Engineering
Volume 5, Issue 5, ISSN (Online): 2249–071X, ISSN (Print): 2278–4209

IV. RESULTS

The proposed system was applied and simulated on the selected data; this data was 15555 examples for training and 5185 examples for testing as specified in the Section (2). The system was carried out on eight kinds of MFs. In order to make a meaningful comparison, the number of MFs for each input, and number of epochs were changed in a linear combination for each MF; see Figs. (A.1-A.10) appendix A. After the training, the obtained best performances of training and test data for each MF at various epochs and number of MFs are listed in Table 2 and shown in Fig. 8. It was noticed that the best three MFs were pimf, gauss2mf and dsigmf. The obtained best ANFIS nets of these functions were reached using 1000, 1000, and 300 epochs with 2, 4, and 3 MFs respectively. Figs. 9-11 show the behavior of the three best MFs before training, while Figs. 12-14 show the behaviour of these functions after training. The performances of the obtained ANFIS nets using the best functions are shown in Fig. 15; error and chkErr are arrays of root mean squared errors representing the training data error signal and the checking data error signal respectively. The chkErr is returned when chkData is supplied as an input argument. The architectures of the best obtained ANFIS systems are shown in Fig. 16.

Three sections were chosen from the studied three images for classifying features; one section from each image. The information of these sections is introduced in Table 3. This system was prepared to form pattern data for these sections to classify dust, cloud, water and vegetation features from their pixels. These sections were selected from area containing the specified features. The proposed colors of classified features are shown in Table 4. The best ANFIS nets of the three MFs were classified the features data from the specified sections precisely. Figs. 17-19 show the selected three sections and their ANFIS nets classification results respectively.

In order to calculate the correct performances of these nets for classifying or mis-classifying features data, four small sections were selected from contiguous areas contained the specified features. One section for each feature was chosen from the three images, except the vegetation feature was not found in contiguous area in the *image1* and *image3*. Fig. 20 shows a sample of these features taken from *image2*. The coordinates of these sections are given in Table 5. The best nets were applied on these sections to classify their pixels as specified features. It was found that the performance of the proposed system was working in powerful process; see Table 4.

Table 2: Performances of proposed system using the eight MFs

	pimf	gauss2mf	dsigmf	posigmf	Gbellmf	gaussmf	trimf	trapmf
No. of MF	2	4	3	3	4	4	4	3
No. epochs	1000	1000	300	300	200	100	100	100
Training Perf.	0.997	0.9957	0.995	0.9954	0.9949	0.9945	0.99	0.9911
Test Perf.	0.99	0.9872	0.986	0.986	0.9849	0.9835	0.98	0.9733

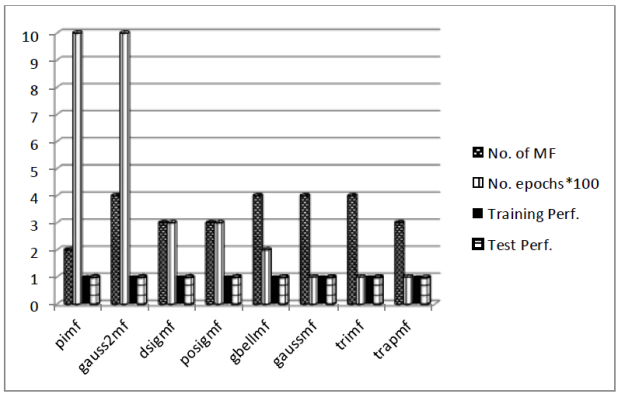

Fig.8. Performances of the training and test data.

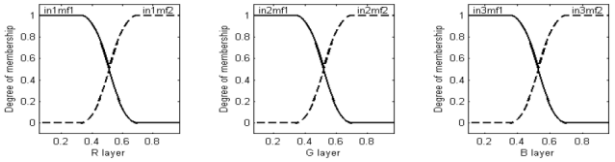

Fig.9. MFs before training by Pimf.

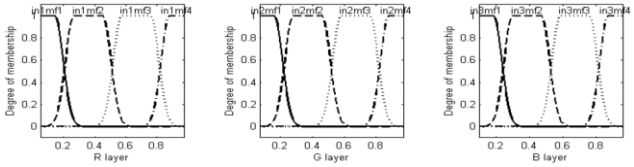

Fig.10. MFs before training by Gauss2mf.

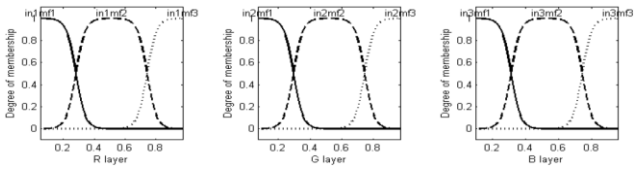

Fig.11. MFs before training by Dsigmf.

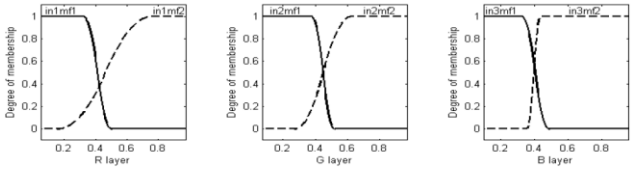

Fig.12. MFs after training by Pimf.

International Journal of Electronics Communication and Computer Engineering
Volume 5, Issue 5, ISSN (Online): 2249–071X, ISSN (Print): 2278–4209

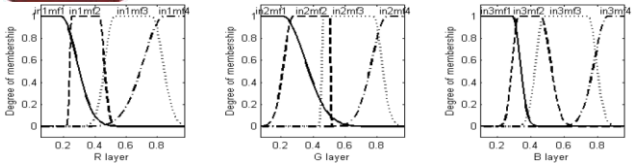

Fig.13. MFs after training by Gauss2mf.

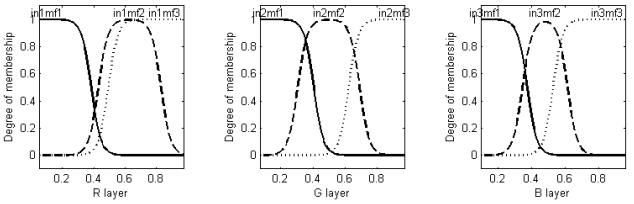

Fig.14. MFs after training by Dsigmf.

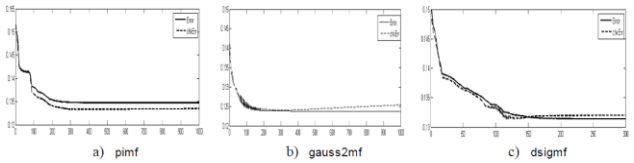

Fig.15. Performances of the obtained ANFIS nets

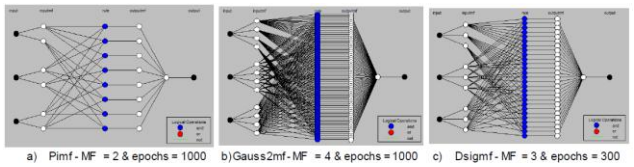

Fig.16. The ANIS architectures of the best nets.

Table 3: The classified sections information

Taken from	Sections Coordinates
image1	2900x300
image2	3210x530
image3	1900x2200

Table 4: The represented colors of classified features

	Cloud
	Light Cloud
	Dust
	Light Dust
	Vegetation
	Light Vegetation
	water

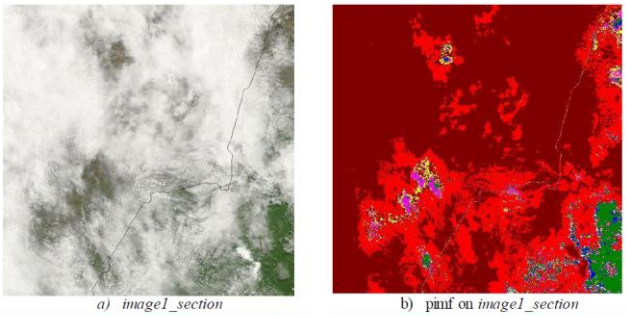

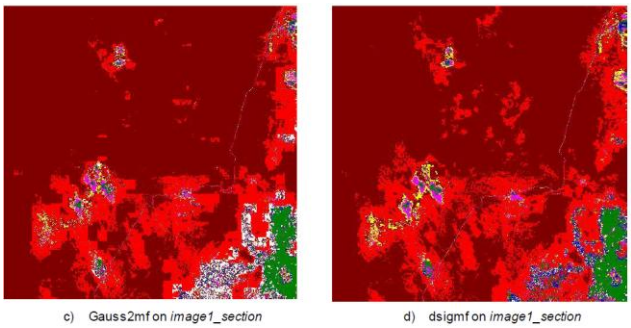

Fig.17. The ANFIS classification results of the section taken from image1

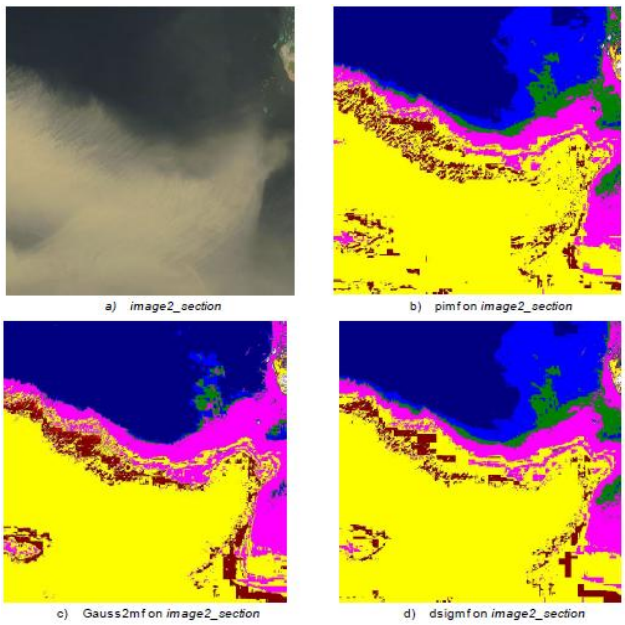

Fig.18. The ANFIS classification results of the section taken from image2

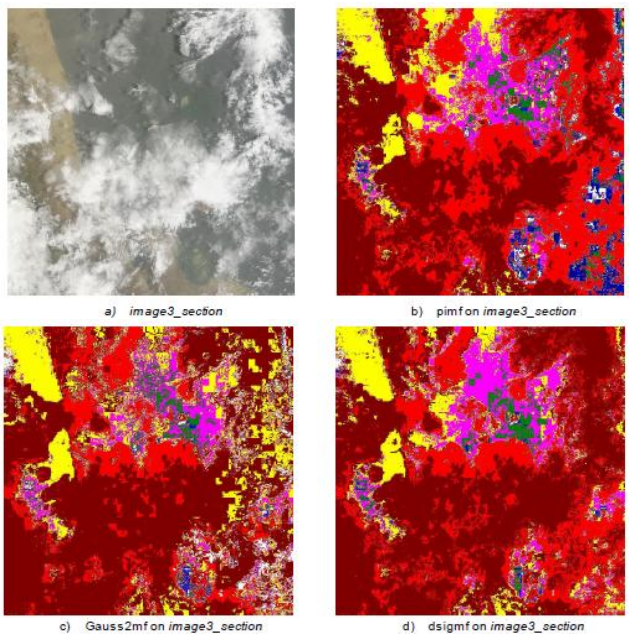

Fig.19. The ANFIS classification results of the section taken from image3

International Journal of Electronics Communication and Computer Engineering
Volume 5, Issue 5, ISSN (Online): 2249–071X, ISSN (Print): 2278–4209

Table 5: The system performances of classified features

Taken from	Section Coordinates & Function Name	Performance			
		dust	clouds	water	vegetation
image1	Coordinates	450x1270	1150x3930	260x130	---
	pimf	%99.81	%100	%99.97	---
	gauss2mf	%99.71	%99.92	%99.83	---
	dsigmf	%99.69	%99.88	%99.64	---
image2	Coordinates	1500x1500	400x2750	1350x350	1360x3360
	pimf	%99.95	%100	%99.76	%100
	gauss2mf	%99.93	%99.87	%99.61	%99.89
	dsigmf	%99.87	%99.86	%99.54	%99.94
image3	Coordinates	520x1660	1280x3320	1150x40	---
	pimf	%99.53	%100	%99.91	---
	gauss2mf	%99.87	%100	%99.85	---
	dsigmf	%99.69	%99.86	%99.85	---

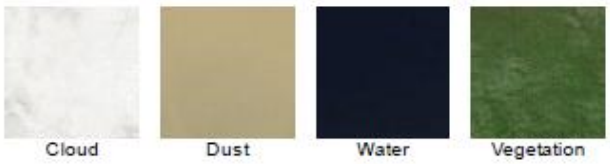

Fig.20. Test images of classified features

V. CONCLUSION

This paper presents ANFIS nets that have the abilities to classify dust, clouds, water and vegetation features from remotely sensed images. They were designed to work in automatic way for finding the best ANFIS net. This system did many tries to find the best ANFIS nets using eight kinds of MFs by changing the number of MFs, and the number of epochs. It was found that, two MFs of pimf kind with 1000 epochs, four MFs of gauss2mf kind with 1000 epochs, or three MFs of dsigmf with 300 epochs were enough for reaching the optimal performance. The performances of these three MFs on the test data were %98.95, %98.72, and %98.62 respectively. Although, the proposed system was trained on data selected only from one image, this system shows an excellent classification of all features in the other two images. Thus, the system can simulate the other data not represented in the training set and classified them correctly. This system can rebuild the architecture of the ANFIS net according to a linear combination among the kind of MF, the number of MF, and number of epochs in automatic way.

APPENDIX

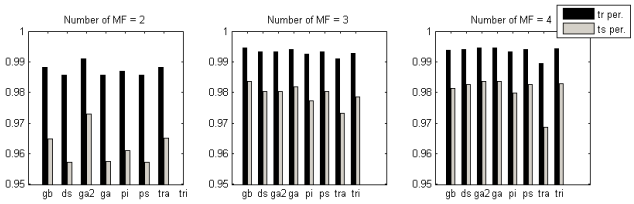

Fig.A.1: Training and test performances at 100

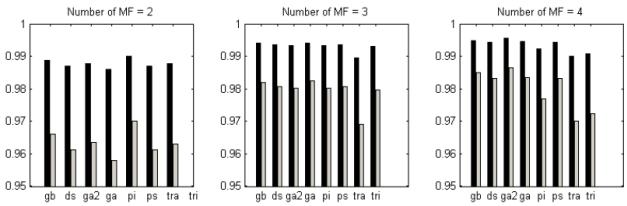

Fig.A.2: Training and test performances at 200

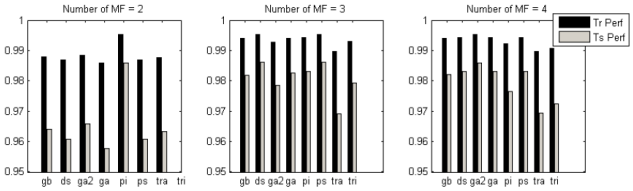

Fig.A.3: Training and test performances at 300

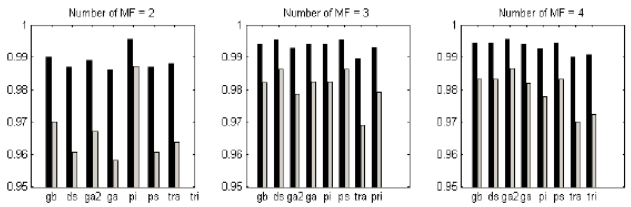

Fig.A.4: Training and test performances at 400

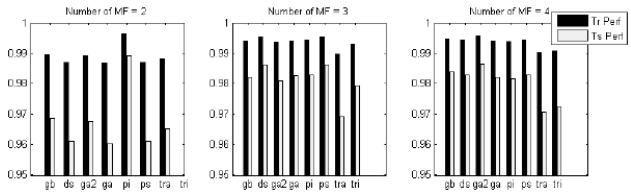

Fig.A.5: Training and test performances at 500

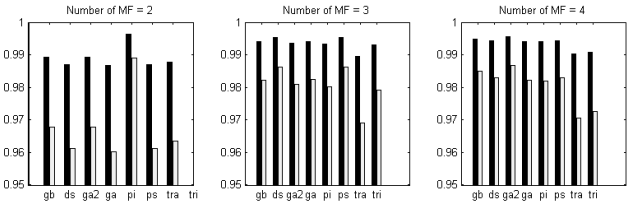

Fig.A.6: Training and test performances at 600

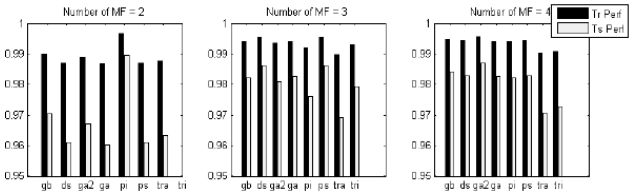

Fig.A.7: Training and test performances at 700

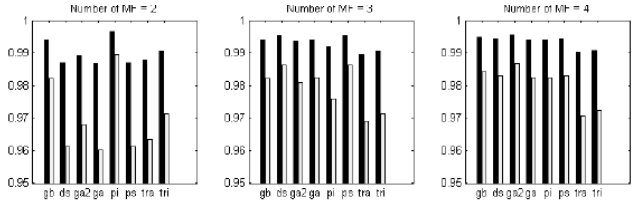

Fig.A.8: Training and test performances at 800

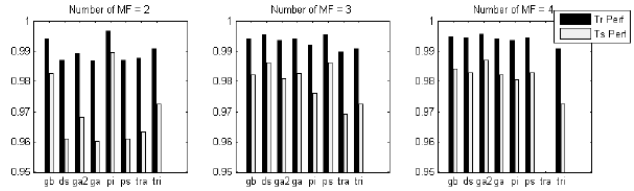

Fig.A.9: Training and test performances at 900

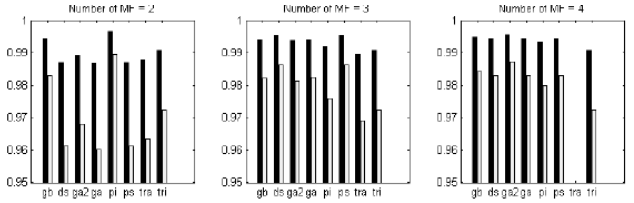

Fig.A.10: Training and test performances at 1000

REFERENCES

[1] Jang J.S.R. Neuro-fuzzy modeling: architecture, analyses and applications. Unpublished Ph.D Dissertation, Department of Electrical Engineering and Computer Science, University of California, Berkeley, California; 1992.

[2] Jang J.S.R. ANFIS: adaptive-network-based fuzzy inference system. IEEE Transaction on Systems, Man and Cybernetics 1993; 23(3):665-685.

[3] Buragohain M., Mahanta C. A novel approach for ANFIS modeling based on full factorial design. Applied Soft Computing archive 2008; 8:609-625.

[4] Ying L.C., Pan M.C. Using adaptive network based fuzzy inference system to forecast regional electricity loads. Energy Conversation and Management 2008; 49:205-211.

[5] Tahmasebi P., Hezarkhani A. Application of a modular feedforward neural network for grade estimation. Natural Resources Research 2011; 20(1):25-32.

[6] Tahmasebi P., Hezarkhani A. Comparison of optimized neural network with fuzzy logic for ore grade estimation. Australian Journal of Basic and Applied Sciences 2010a; 4(5):764-772.

[7] Tahmasebi P., Hezarkhani A. Application of adaptive neuro-fuzzy inference system for grade estimation; case study, sarcheshmeh porphyry copper deposit, Kerman, Iran. Australian Journal of Basic and Applied Sciences 2010b; 4(3):408-420.

[8] Alfonso I., Carlos D., Bernardino A., Manuel C. J. Integration of remote sensing techniques and connectionist models for decision support in fishing catches. Environmental Modelling & Software 2007; 22:862-870.

[9] Hui L., Pei L., Junshi X., Huasheng S., Kun T., Shuwei D. Research on Technology for Land Use Map renewal and Database Construction, Procedia Environmental Sciences 2011; 11:706-712.

[10] Bai L., Lin H., Sun H., Zang Z., Mo. D. Remotely Sensed Percent Tree Cover Mapping Using Support Vector Machine Combined with Autonomous Endmember Extraction. Physics Procedia 2012; 33:1702-1709.

[11] Roberts J., Tesfamichael S., Gebreslasie M., Aardt J., Ahmed F. Forest structural assessment using remote sensing technologies: an overview of the current state of the art. Southern Hemisphere Forestry Journal 2007;69(3):183-203.

[12] Choi M., Jacobs J. M., Anderson M. C., Bosch D. D. Evaluation of drought indices via remotely sensed data with hydrological variables. Journal of Hydrology 2013; 476:265-273.

[13] Abd El-Kawy O.R., Rød J.K., Ismail H.A., Suliman A.S. Land use and land cover change detection in the western Nile delta of Egypt using remote sensing data. Applied Geography 2011; 31(2):483-494.

[14] Thenkabail P. S., Schull M., Turral H. Ganges and Indus river basin land use/land cover (LULC) and irrigated area mapping using continuous streams of MODIS data. Remote Sensing of Environment 2005; 95(3):317-341.

[15] Pradhan B., Sezer E. A., Gokceoglu C., Buchroithner M. F. Landslide Susceptibility Mapping By Neuro-Fuzzy Approach In A Landslide-Prone Area (Cameron Highlands, Malaysia). Ieee Transactions On Geoscience And Remote Sensing 2010; 48 (12).

[16] Sezer E. A., Pradhan B., Gokceoglu C. Manifestation of an adaptive neuro-fuzzy model on landslide susceptibility mapping: Klang valley, Malaysia. Expert Systems with Applications 2011; 38:8208-8219.

[17] Oh H.-J., Pradhan B. Application of a neuro-fuzzy model to landslide-susceptibility mapping for shallow landslides in a tropical hilly area. Computers & Geosciences 2011; 37:1264-1276.

[18] Pradhan B. A comparative study on the predictive ability of the decision tree, support vector machine and neuro-fuzzy models in landslide susceptibility mapping using GIS. Computers & Geosciences 2013; 51:350-365.

[19] Song K.-Y., Oh H.-J., Choi J., Park I., Lee C., Lee S. Prediction of landslides using ASTER imagery and data mining models. Advances in Space Research 2012; 49:978-993.

[20] Stathakis D., Vasilakos At. Comparison Of Computational Intelligence Based Classification Techniques For Remotely Sensed Optical Image Classification. Ieee Transactions On Geoscience And Remote Sensing 2006; 44(8).

[21] Halder A., Ghosh A., Ghosh S. Supervised and unsupervised landuse map generation from remotely sensed images using ant based systems. Applied Soft Computing 2011; 11:5770-5781.

[22] Kamarianakis Y., Feidas H., Kokolatos G., Chrysoulakis N., Karatzias V. Evaluating remotely sensed rainfall estimates using nonlinear mixed models and geographically weighted regression. Environmental Modelling & Software 2008; 23:1438-1447.

[23] Halder A., Ghosh A., Ghosh S. Supervised and unsupervised landuse map generation from remotely sensed images using ant based systems. Applied Soft Computing 2011; 11:5770-5781.

[24] Kamarianakis Y., Feidas H., Kokolatos G., Chrysoulakis N., Karatzias V. Evaluating remotely sensed rainfall estimates using nonlinear mixed models and geographically weighted regression. Environmental Modelling & Software 2008; 23:1438-1447.

[25] Foody G. M. Assessing the accuracy of land cover change with imperfect ground reference data. Remote Sensing of Environment 2010; 114(10), 2271-2285.

[26] Kuplich T. M. Classifying regenerating forest stages in Amazoˆnia using remotely sensed images and a neural network. Forest Ecology and Management 2006; 234:1-9.

[27] Ren Y., Yan J., Wei X., Wang Y., Yang Y., Hua L., Xiong Y., Niu X., Song X. Effects of rapid urban sprawl on urban forest carbon stocks: Integrating remotely sensed, GIS and forest inventory data. Journal of Environmental Management 2012; 113:447-455.

[28] Franklin J., Spears-Lebrun L. A., Deutschman D.H., Marsden K. Impact of a high-intensity fire on mixed evergreen and mixed conifer forests in the Peninsular Ranges of southern California. USA. Forest Ecology and Management 2006; 235(1-3):18-29.

[29] Schwarz J. N., Raymond B., Williams G.D., Pasquer B. D., Marsland S. J., Gorton R.J. Biophysical coupling in remotely-sensed wind stress, sea surface temperature, sea ice and chlorophyll concentrations in the South Indian Ocean. Deep-Sea Research II 2010; 57:701-722.

[30] Padin X. A., Navarro G., Gilcoto M., Rios A.F., Pérez F.F. Estimation of air-sea CO2 fluxes in the Bay of Biscay based on empirical relationships and remotely sensed observations. Journal of Marine Systems 2009; 75:280-289.
[31] Ling F., Li X., Xiao F., Fang S., Du Y. Object-based sub-pixel mapping of buildings incorporating the prior shape information from remotely sensed imagery. International Journal of Applied Earth Observation and Geoinformation 2012; 18:283-292.
[32] Adegoke J. O., Pielke R., Carleton A. M. Observational and modeling studies of the impacts of agriculture-related land use change on planetary boundary layer processes in the central U.S. Agricultural and Forest Meteorology 2007; 142(2-4):203-215.
[33] Qi J., Kerr Y. H., Moran M. S., Weltz M., Huete A. R., Sorooshian S., Bryant R. Leaf Area Index Estimates Using Remotely Sensed Data and BRDF Models in a Semiarid Region. Remote Sens. Environ. 2000; 73:18-30.
[34] Nasahara K. N., Muraoka H., Nagai S., Mikami H. Vertical integration of leaf area index in a Japanese deciduous broad-leaved forest. agricultural and forestmeteorology. 2008;148:1136-1146.
[35] Qiao W., Rong J., Zhong X. An adaptive neural-fuzzy-based multi-sensor data fusion architecture for target tracking systems. International Journal of Remote Sensing 2009; 30(18):4897-4904.
[36] Song K.-Y., Oh H.-J., Choi J., Park I., Lee C., Lee S. Prediction of landslides using ASTER imagery and data mining models. Advances in Space Research 2012; 49:978–993.
[37] Subasi A. Application of adaptive neuro-fuzzy inference system for epileptic seizure detection using wavelet feature extraction. Computers in Biology and Medicine2007; 37:227-244,.
[38] Oh H.-J., Pradhan . Application of a neuro-fuzzy model to landslide-susceptibility mapping for shallow landslides in a tropical hilly area. Computers & Geosciences 2011; 37:1264-1276.
[39] Binaghi E., Gallo I., Madella P. A neural model for fuzzy Dempster-Shafer classifiers. International Journal of Approximate Reasoning 2000; 25:89-121.
[40] Sevastianov P., Dymova L. Synthesis of fuzzy logic and Dempster-Shafer Theory for the simulation of the decision-making process in stock trading systems. Mathematics and Computers in Simulation 2009; 80:506-521.
[41] Ajil K .S., Thapliyal P. K., Shukla, Pal P. K., Joshi P. C., Navalgund R. R. A New Technique for Temperature and Humidity Profile Retrieval From Infrared-Sounder Observations Using the Adaptive Neuro-Fuzzy Inference System. Geoscience and Remote Sensing, IEEE Transactions on, Issue Date: April 2010.
[42] Polat K., Guenes S. Automated identification of diseases related to lymph system from lymphography data using artificial immune recognition system with fuzzy resource allocation mechanism (fuzzy-AIRS). Biomedical Signal Processing and Control 2006; 1:253-260,.
[43] Polat K., Sahan S., Guenes S. Automatic detection of heart disease using an artificial immune recognition system (AIRS) with fuzzy resource allocation mechanism and k-nn (nearest neighbour) based weighting preprocessing. Expert Systems with Applications 2007; 32:625-631.
[44] Lin C.-J. An efficient immune-based symbiotic particle swarm optimization learning algorithm for TSK-type neuro-fuzzy networks design. Fuzzy Sets and Systems 2008;159:2890-2909.
[45] Lin C.-J., Liu Y.-C. Image backlight compensation using neuro-fuzzy networks with immune particle swarm optimization. Expert Systems with Applications 2009; 36:5212-5220.
[46] Shen J., Shen W., Sun H.J., Yang J.Y. Fuzzy neural nets with non-symmetric p MFs and applications in signal processing and image analysis. Signal Processing 2000; 80:965-983.
[47] Atsalakis G. S., Valavanis K. P. Surveying stock market forecasting techniques-Part II: Soft computing methods. Expert Systems with Applications 2009; 36: 5932-5941.
[48] Fuzzy Logic Toolbox For Use with MATLAB, http://ssdi.di.fct.unl.pt/scl/docs/texts/fuzzy%20logic.
[49] http://www.eoimages.gsfc.nasa.gov/images/imagerecords/44000/44777/redsea_tmo_2010205_lrg.jpg
[50] http://www.eoimages.gsfc.nasa.gov/images/imagerecords/51000/51414/redsea_tmo_2011201_lrg.jpg
[51] http://www.eoimages.gsfc.nasa.gov/images/imagerecords/51000/51593/redsea_tmo_2011215_lrg.jpg
[52] Oh H.-J., Pradhan B. Application of a neuro-fuzzy model to landslide-susceptibility mapping for shallow landslides in a tropical hilly area. Computers & Geosciences 2011; 37:1264-1276.

AUTHOR'S PROFILE

G. M. Behery
is an associative professor ofComputer Science in the Department of Mathematics and Computer Science, DamiettaUniversity, Faculty of Science. He received his B.Sc. degree in Computer Science from the Faculty of science, Suez Canal University, his M.Sc. degree in computer science from Damietta, faculty of science at Mansoura University, and Ph.D. in computer science from Germany/Egypt (Friedrich-Alexander-Universität Erlangen-Nürnberg/Mansoura University). His research interests include neural networks, image processing, artificial intelligent, fuzzy logic, data structure, and OS. Address: Department of Maths., Faculty of Science, Damietta University, New Damietta 34517.
Email: behery2911961@yahoo.com.